# First observation and branching fraction measurement of the $\Lambda_b^0 \to D_s^- p$ decay

## The LHCb collaboration

*E-mail:* maciej.artur.giza@cern.ch

ABSTRACT: The first observation of the $\Lambda_b^0 \to D_s^- p$ decay is presented using proton-proton collision data collected by the LHCb experiment at a centre-of-mass energy of $\sqrt{s} = 13\,\text{TeV}$, corresponding to a total integrated luminosity of $6\,\text{fb}^{-1}$. Using the $\Lambda_b^0 \to \Lambda_c^+ \pi^-$ decay as the normalisation mode, the branching fraction of the $\Lambda_b^0 \to D_s^- p$ decay is measured to be $\mathcal{B}(\Lambda_b^0 \to D_s^- p) = (12.6 \pm 0.5 \pm 0.3 \pm 1.2) \times 10^{-6}$, where the first uncertainty is statistical, the second systematic and the third due to uncertainties in the branching fractions of the $\Lambda_b^0 \to \Lambda_c^+ \pi^-$, $D_s^- \to K^- K^+ \pi^-$ and $\Lambda_c^+ \to p K^- \pi^+$ decays.

# Contents

## 1   Introduction

The Standard Model (SM) of particle physics describes the elementary particles and their interactions. In the SM, the Cabibbo-Kobayashi-Maskawa (CKM) mechanism describes how the weak interaction eigenstates are related to the mass eigenstates of the quarks and, therefore, also describes the interaction strengths among quarks via the weak interaction [1, 2]. The CKM-matrix element describing the $b \to u$ transition, $V_{ub}$, is the element with the smallest and most poorly determined magnitude. Better knowledge on $|V_{ub}|$ provides a critical input to check the consistency of the SM [3, 4].

The $\Lambda_b^0 \to D_s^- p$ decay[1] is a weak hadronic decay that proceeds through a $b \to u$ transition. A single leading-order diagram contributes to this process, shown in figure 1. Therefore, the $\Lambda_b^0 \to D_s^- p$ branching fraction is proportional to $|V_{ub}|^2$,

$$\mathcal{B}(\Lambda_b^0 \to D_s^- p) \propto |V_{ub}|^2 |V_{cs}|^2 f_{D_s}^2 |a_{NF}|^2 |F_{\Lambda_b^0 \to p}(m_{D_s}^2)|^2 \,, \tag{1.1}$$

where $|V_{cs}|$ describes the $c \to s$ quark transition, $f_{D_s}$ is the $D_s^-$ decay constant, $F_{\Lambda_b^0 \to p}$ is the form factor describing the $\Lambda_b^0$ to proton transition and $|a_{NF}|$ quantifies the nonfactorisable effects, *i.e.* final-state strong interactions leading to a nonfactorisable contribution in the decay amplitude. The $f_{D_s}$ constant has been calculated with high precision using lattice QCD [5, 6] and $|V_{cs}|$ is known to be close to unity [7]. Describing a heavy-quark decay as the product of the matrix elements of two currents is known as factorisation and leads to

---

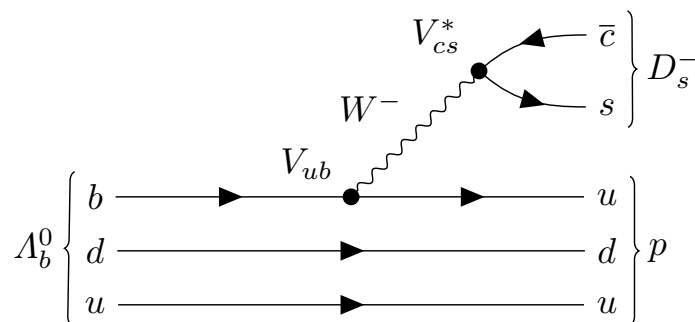[1]Inclusion of charge-conjugated modes is implied unless explicitly stated.

**Figure 1**. Tree diagram contributing to the $\Lambda_b^0 \to D_s^- p$ decay.

the product of the decay constant and the form factor. Factorisation is expected to be a good approximation if the emitted meson is light relative to the other hadron, formed from the spectator quarks [8]. Therefore, factorisation may not hold in the $\Lambda_b^0 \to D_s^- p$ decay, where the $D_s^-$ meson is heavier than the proton.

The calculations of the matrix elements simplify in semileptonic decays, where they are the product of the leptonic and the hadronic currents. Therefore, semileptonic decays are used to determine $|V_{ub}|$, where the hadronic matrix elements can be calculated using nonperturbative methods. By contrast, the knowledge of the matrix elements in hadronic decays is poorly known, as they are plagued by nonfactorisable effects in the final state. Recently, the branching fraction of the $B^0 \to D_s^+ \pi^-$ decay has been measured [9]. The $B^0 \to D_s^+ \pi^-$ decay proceeds with the same tree-level transition as the $\Lambda_b^0 \to D_s^- p$ decay, leading to the same expression as eq. (1.1), except for the form factor and nonfactorisable effects. For the $B^0 \to D_s^+ \pi^-$ decay, the form factor is known with about 10% precision [10, 11], which allows for the determination of the product of $|V_{ub}|$ and $|a_{NF}|$. The $\Lambda_b^0 \to D_s^- p$ decay can, in principle, provide another measure of the breaking of the factorisation hypothesis. However, the form factor for this decay is not accurately known yet [12]. Therefore, this measurement provides an incentive to address these calculations.

This paper presents the first observation and branching fraction measurement of the $\Lambda_b^0 \to D_s^- p$ decay using proton-proton ($pp$) collision data collected with the LHCb detector at a centre-of-mass energy of 13 TeV and corresponding to an integrated luminosity of 6 fb$^{-1}$. Data taken in Run 2 of the Large Hadron Collider (LHC) between 2015 and 2018 is used. The $\Lambda_b^0 \to \Lambda_c^+ \pi^-$ decay is used as a normalisation channel because it is topologically similar to the signal decay and has a relatively high branching fraction. Candidates of $\Lambda_b^0 \to D_s^- p$ ($\Lambda_b^0 \to \Lambda_c^+ \pi^-$) decays are reconstructed using the final-state particles of the $D_s^- \to K^- K^+ \pi^-$ ($\Lambda_c^+ \to pK^- \pi^+$) decay. The branching fraction of $\Lambda_b^0 \to D_s^- p$ is determined using

$$\mathcal{B}(\Lambda_b^0 \to D_s^- p) = \mathcal{B}(\Lambda_b^0 \to \Lambda_c^+ \pi^-) \frac{N_{\Lambda_b^0 \to D_s^- p}}{N_{\Lambda_b^0 \to \Lambda_c^+ \pi^-}} \frac{\epsilon_{\Lambda_b^0 \to \Lambda_c^+ \pi^-}}{\epsilon_{\Lambda_b^0 \to D_s^- p}} \frac{\mathcal{B}(\Lambda_c^+ \to pK^- \pi^+)}{\mathcal{B}(D_s^- \to K^- K^+ \pi^-)}, \qquad (1.2)$$

where $N_X$ is the measured yield of decay $X$ and $\epsilon_X$ is the efficiency of the candidate reconstruction and selection. The candidate yields are determined using unbinned extended maximum-likelihood fits of the invariant mass of the $\Lambda_b^0$ hadron. The corresponding efficiencies are determined using simulated candidates and calibration data samples.

## 2   Detector and simulation

The LHCb detector [13, 14] is a single-arm forward spectrometer covering the pseudorapidity range $2 < \eta < 5$, designed for the study of particles containing $b$ or $c$ quarks. The detector includes a high-precision tracking system consisting of a silicon-strip vertex detector surrounding the $pp$ interaction region, a large-area silicon-strip detector located upstream of a dipole magnet with a bending power of about $4\,\mathrm{Tm}$, and three stations of silicon-strip detectors and straw drift tubes placed downstream of the magnet. The tracking system provides a measurement of the momentum, $p$, of charged particles with a relative uncertainty that varies from $0.5\%$ at low momentum to $1.0\%$ at $200\,\mathrm{GeV}/c$. The minimum distance of a track to a primary $pp$ collision vertex (PV), the impact parameter (IP), is measured with a resolution of $(15 + 29/p_\mathrm{T})\,\mu\mathrm{m}$, where $p_\mathrm{T}$ is the component of the momentum transverse to the beam, in $\mathrm{GeV}/c$. Different types of charged hadrons are distinguished using information from two ring-imaging Cherenkov detectors. Photons, electrons and hadrons are identified by a calorimeter system consisting of scintillating-pad and preshower detectors, an electromagnetic and a hadronic calorimeter. Muons are identified by a system composed of alternating layers of iron and multiwire proportional chambers. The online event selection is performed by a trigger, which consists of a hardware stage, based on information from the calorimeter and muon systems, followed by a software stage, which applies a full event reconstruction. At the hardware trigger stage, events are required to have a muon with high $p_\mathrm{T}$ or a hadron, photon or electron with high transverse energy in the calorimeters. For hadrons, the transverse energy threshold is $3.5\,\mathrm{GeV}$. Events selected by the hadron trigger or by any other trigger independently of the signal candidate are used in this analysis. The software trigger requires a two-, three- or four-track secondary vertex with a significant displacement from any primary $pp$ interaction vertex. At least one charged particle must have a transverse momentum $p_\mathrm{T} > 1.6\,\mathrm{GeV}/c$ and be inconsistent with originating from a PV. A multivariate algorithm [15, 16] is used for the identification of secondary vertices consistent with the decay of a $b$ hadron.

Simulation is required to calculate reconstruction and selection efficiencies, and to determine shapes of invariant-mass distributions. In the simulation, $pp$ collisions are generated using PYTHIA [17] with a specific LHCb configuration [18]. Decays of unstable particles are described by EVTGEN [19], in which final-state radiation is generated using PHOTOS [20]. The interaction of the generated particles with the detector, and its response, are implemented using the GEANT4 toolkit [21, 22] as described in ref. [23].

## 3   Selection of candidates

The $\Lambda_b^0 \to D_s^- p$ ($\Lambda_b^0 \to \Lambda_c^+ \pi^-$) decay is reconstructed by selecting $D_s^- \to K^- K^+ \pi^-$ ($\Lambda_c^+ \to p K^- \pi^+$) candidates and combining them with a proton (charged pion), which is referred to as the companion particle. A kinematic fit [24] is used to improve the $\Lambda_b^0$ mass resolution by constraining the $D_s^-$ ($\overline{\Lambda}_c^-$) mass to its known value [7]. The $D_s^- p$ ($\Lambda_c^+ \pi^-$) invariant mass, $m(D_s^- p)$ ($m(\Lambda_c^+ \pi^-)$), is required to be within the range 5200–6200 (5400–6200) $\mathrm{MeV}/c^2$ and the unconstrained $K^- K^+ \pi^-$ ($\overline{p} K^+ \pi^-$) invariant mass must be within 1948–1988 (2266–2306) $\mathrm{MeV}/c^2$.

Candidates that have been selected by the trigger requirements, as described in the previous section, are subject to further offline selection to reduce the background contributions. First, a preselection reconstructs $b$-hadron and $c$-hadron candidates with good-quality vertices by reconstructing four well-reconstructed tracks with high transverse and total momentum and inconsistent with originating from any PV. A gradient-boosted decision tree (BDTG) algorithm [25, 26] is used to reduce the background contributions due to random combinations of final-state particles. This BDTG classifier is trained on $B_s^0 \to D_s^- \pi^+$ candidates taken in 2011 and 2012 (Run 1) and is described in ref. [27]. The BDTG is suitable for decays topologically similar to $B_s^0 \to D_s^- \pi^+$, as it does not use particle identification variables. The BDTG classifier combines a number of track-related variables, including the transverse momentum of the companion particle, the $b$-hadron and $c$-hadron candidate's radial flight distance and the companion and $b$ hadron's minimum $\chi_{\mathrm{IP}}^2$, where $\chi_{\mathrm{IP}}^2$ is defined as the difference in the vertex-fit $\chi^2$ of the PV reconstructed with and without the candidate. A more detailed description of the BDTG classifier is given in ref. [28]. It has been verified using $\Lambda_b^0 \to D_s^- p$ simulation that this BDTG performs well in separating signal from combinatorial background.

To separate $\Lambda_b^0 \to D_s^- p$ from backgrounds with a misidentified final-state particle, a requirement on the PID of the companion proton is applied. This requirement is based on multivariate techniques to combine the PID and tracking information of all LHCb subsystems to get a single discriminating variable [29]. The optimal requirements for the BDTG classifier and the companion identification variables are simultaneously determined by maximising the figure of merit $\epsilon_{\mathrm{sig}}/(5 + \sqrt{N_{\mathrm{bg}}})$ [30] expected for the signal region ($m(D_s^- p) \in [5580, 5660]\,\mathrm{MeV}/c^2$). Here, $\epsilon_{\mathrm{sig}}$ is the signal efficiency of the corresponding BDTG and PID requirements in addition to the other selection requirements, and $N_{\mathrm{bg}}$ is the expected number of background events in the signal region for the given set of selection requirements. The optimal point of this figure of merit corresponds to a tight PID requirement on the companion proton with a signal efficiency of 76%, calculated after applying the other selection requirements. For the $\Lambda_b^0 \to \Lambda_c^+ \pi^-$ sample, similar to the signal sample, a PID requirement is imposed on the companion pion to remove contributions from $\Lambda_b^0 \to \Lambda_c^+ K^-$ decays.

To further reduce contributions of backgrounds due to misidentification of the final-state particles, PID requirements are imposed on the decay products of the $c$-hadron. Furthermore, vetoes are applied to the $D_s^\mp h^\pm$ samples to reduce the contribution from $D^- \to K^+ \pi^- \pi^-$ and $\Lambda_c^+ \to p K^- \pi^+$ decays misidentified as $D_s^- \to K^- K^+ \pi^-$ candidates. In these vetoes, the $D_s^-$ candidates are reconstructed as $D^- \to K^+ \pi^- \pi^-$ or $\Lambda_c^+ \to p K^- \pi^+$ decays, and a tight PID requirement is imposed on those near the known $D^-$ or $\bar{\Lambda}_c^-$ mass. The PID requirements together have a signal efficiency of 56% for the $\Lambda_b^0 \to D_s^- p$ sample and 71% for the $\Lambda_b^0 \to \Lambda_c^+ \pi^-$ sample, calculated after applying the other selection requirements. Finally, contributions from $b$-hadron decays not including a charm hadron are suppressed by a requirement on the $c$-hadron's flight-distance significance, defined as the distance between the $b$- and $c$-hadron decay vertices divided by the uncertainty on this measurement. This requirement is applied to all samples.

The efficiency of the candidate selection is calculated using simulated $\Lambda_b^0 \to D_s^- p$ and $\Lambda_b^0 \to \Lambda_c^+ \pi^-$ decays, except for the PID and hardware-trigger efficiencies, which are

| Requirement | Ratio $\epsilon(\Lambda_b^0 \to \Lambda_c^+ \pi^-)/\epsilon(\Lambda_b^0 \to D_s^- p)$ |
|---|---|
| LHCb acceptance | $0.9625 \pm 0.0016$ |
| Software trigger and preselection | $1.1370 \pm 0.0026$ |
| Kinematic and geometric selection | $0.7580 \pm 0.0018$ |
| Particle identification selection | $1.278 \ \pm 0.005$ |
| Hardware trigger | $0.995 \ \pm 0.006$ |
| Total | $1.070 \ \pm 0.010$ |

**Table 1**. A breakdown of the relative efficiency ratios of the $\Lambda_b^0 \to \Lambda_c^+ \pi^-$ and $\Lambda_b^0 \to D_s^- p$ decays, calculated after applying the preceding requirements. The uncertainty on the efficiencies is due to the size of the simulation and calibration samples.

determined using calibration data samples. The efficiency of the PID requirements is calculated using samples of $D^{*+} \to D^0 \pi^+$ and $\Lambda_c^+ \to pK^- \pi^+$ calibration data. A more complete description of this method can be found in ref. [31]. The determination of the hardware trigger efficiency uses the $D^{*+} \to D^0 \pi^+$ and $\Lambda^0 \to p\pi^-$ calibration samples and simulated signal. The efficiencies of hadrons to be triggered depend on and therefore are calibrated based on the type and charge of the particle, as well as the magnitude and the calorimeter region, demarcated by the cell sizes, of the corresponding energy deposit in the calorimeter. Table 1 shows the ratio of the selection efficiencies between the signal and normalisation channels. The most sizeable differences in efficiency are due to the different PID requirements for the signal and normalisation channel and due to the flight-distance significance and momentum requirements.

Two control channels, $B_s^0 \to D_s^- \pi^+$ and $B_s^0 \to D_s^\mp K^\pm$, are used to estimate the contributions of misidentified $B_s^0 \to D_s^{(*)-}\{\pi^+, \rho^+\}$ and $B_{(s)}^0 \to D_s^{(*)\mp} K^{(*)\pm}$ decays in the $\Lambda_b^0 \to D_s^- p$ sample. The control modes are subjected to the same candidate selection as $\Lambda_b^0 \to D_s^- p$ candidates, except for the particle identification (PID) requirement on the companion particle.

## 4   Invariant-mass fits

The yields of the signal $\Lambda_b^0 \to D_s^- p$ and normalisation $\Lambda_b^0 \to \Lambda_c^+ \pi^-$ channels are determined using unbinned maximum-likelihood fits to the $D_s^- p$ and $\Lambda_c^+ \pi^-$ invariant-mass distributions, respectively. The candidate samples from different years of data-taking and magnet polarities are combined in the fits.

The signal components in the invariant-mass fits are parameterised using the sum of a double-sided Hypatia function [32] and a Johnson $S_U$ function [33]. Their corresponding parameters are obtained from fits to samples of simulated candidates. In the fit to $\Lambda_b^0 \to \Lambda_c^+ \pi^-$ candidates in data, the common mean of the functions and the widths are left unconstrained to account for any under- or overestimation of resolution effects in the simulation. The widths from the fit to $\Lambda_b^0 \to \Lambda_c^+ \pi^-$ candidates, scaled with the expected width differences from simulation, are used to fix the widths in the fit to $\Lambda_b^0 \to D_s^- p$ candidates, where only the mean is left unconstrained.

The residual combinatorial background contribution is modelled using analytic functions. In the $m(D_s^- p)$ fit, this contribution is parametrised as $\mathcal{C}(m|m_0, A, C) = (1 - \exp(-(m - m_0)/C)) \times (m/m_0)^A$, which describes the turn-on point in the $D_s^- p$ invariant-mass due to $D_s^- \pi^+$ invariant-mass requirements in the preselection. The parameters of this function are determined by fitting the $m(D_s^- p)$ distribution using the upper sideband region of $m(K^- K^+ \pi^-)$ and are subsequently fixed in the fit to data. In the $m(\Lambda_c^+ \pi^-)$ fit, the combinatorial background is described using an exponential distribution, validated on the upper $m(\Lambda_c^+ \pi^-)$ sideband. The exponential parameter is left unconstrained in the fit to account for kinematic differences between the $m(\Lambda_c^+ \pi^-)$ sideband and the full range.

Decays where one or more of the final-state particles are missed by the reconstruction are referred to as partially reconstructed backgrounds. In the fits to the signal and normalisation channels, these backgrounds are parametrised by parabolic functions convolved with a double Gaussian distribution to account for detector effects. These functions describe decays where a neutral pion or photon is not reconstructed [34]. The fit to $\Lambda_b^0 \to D_s^- p$ candidates considers partially reconstructed background components from $\Lambda_b^0 \to D_s^{*-}(\to D_s^- \gamma/\pi^0)p$ decays. As the $D_s^{*-}$ meson decays to either $D_s^- \gamma$ or to $D_s^- \pi^0$, this contribution is described by a combination of two of the above-mentioned parabolic functions. The corresponding parameters are obtained from simulation and fixed in the fit to data. The yield of $\Lambda_b^0 \to D_s^{*-} p$ decays is left unconstrained in the fit to $\Lambda_b^0 \to D_s^- p$ candidates, as there is no estimate of the corresponding branching fraction. The addition of an extra partially reconstructed component describing $\Lambda_b^0 \to D_s^- \Delta^+$ decays has been studied and is found to have a negligible impact on the signal yield. The $\Lambda_b^0 \to \Lambda_c^+ \pi^-$ sample contains partially reconstructed backgrounds from $\Lambda_b^0 \to \Lambda_c^+ \rho^-(\to \pi^- \pi^0)$ and $\Lambda_b^0 \to \Sigma_c^+(\to \Lambda_c^+ \pi^0)\pi^-$ decays. These are both parametrised using a parabolic function to describe the missing neutral pion. The parameters of this function are obtained from simulation and fixed in the $m(\Lambda_c^+ \pi^-)$ fit, while the yields are left free.

The background contributions due to the misidentification of the companion particle in the $m(D_s^- p)$ fit consist of the decays $B_s^0 \to D_s^- \pi^+$, $B_s^0 \to D_s^\mp K^\pm$, $B^0 \to D_s^- K^+$ and the corresponding backgrounds with missing photons or neutral pions in the final state, originating from $\rho^+ \to \pi^+ \pi^0$, $K^{*+} \to K^+ \pi^0$ or $D_s^{*-} \to D_s^- \{\gamma, \pi^0\}$ decays. The shapes of the misidentified backgrounds in the $m(D_s^- p)$ fit are determined from simulation using a nonparametric kernel estimation method [35]. The exceptions are the $B_s^0 \to D_s^{*-} \pi^+$ and $B^0 \to D_s^{*-} \pi^+$ components, described by Crystal Ball functions [36]. The shape of the $B_s^0 \to D_s^{*-} \pi^+$ contribution is obtained from simulation. The same parametrisation shifted by the known $B^0$–$B_s^0$ mass difference is used to model $B^0 \to D_s^{*-} \pi^+$ decays. All misidentified backgrounds have fixed shapes in the fit to the $D_s^- p$ invariant mass. Fits to the $B_s^0$ invariant mass in the $B_s^0 \to D_s^- \pi^+$ and $B_s^0 \to D_s^\mp K^\pm$ control samples (see appendix B) provide an estimate of the contributions of the misidentified background components in the $\Lambda_b^0 \to D_s^- p$ sample. These estimates are computed by correcting the observed yields of $B_s^0 \to D_s^{(*)-}\{\pi^+, \rho^+\}$ and $B_{(s)}^0 \to D_s^{(*)\mp} K^{(*)\pm}$ decays for the different PID requirements between the control and signal samples. Subsequently, they are constrained in the $m(D_s^- p)$ fit.

The sample of $\Lambda_b^0 \to \Lambda_c^+ \pi^-$ candidates is contaminated by the $\Lambda_b^0 \to \Lambda_c^+ K^-$, $B_s^0 \to D_s^- \pi^+$ and $B^0 \to D^- \pi^+$ backgrounds due to the misidentification of one of the final-state particles. The shapes of these backgrounds are determined from simulation using a nonparametric kernel estimation method and fixed in the fit to data. The size of the $\Lambda_b^0 \to \Lambda_c^+ K^-$ contribution is constrained to the expected yield determined using knowledge of its branching fraction [37] and efficiencies obtained from simulation. A data-driven method is used to determine the $B_s^0 \to D_s^- \pi^+$ and $B^0 \to D^- \pi^+$ yields in the $m(\Lambda_c^+ \pi^-)$ fit. The $\Lambda_c^+ \pi^-$ data is reconstructed as $D_s^- \pi^+$ and $D^- \pi^+$, fitted, and the resulting yields are corrected for the difference in PID and invariant-mass requirements. Ultimately, the number of expected $B_s^0 \to D_s^- \pi^+$ and $B^0 \to D^- \pi^+$ is small and is therefore fixed in the fit to $\Lambda_b^0 \to \Lambda_c^+ \pi^-$ candidates.

The $\Lambda_c^+ \pi^-$ invariant-mass distribution and the fit projection of the $\Lambda_b^0 \to \Lambda_c^+ \pi^-$ signal and the background components are shown in figure 2. The $\Lambda_b^0 \to \Lambda_c^+ \pi^-$ yield obtained from this fit is $404\,700 \pm 700$, where the uncertainty is statistical.

Finally, the fit to the invariant-mass distribution of $\Lambda_b^0 \to D_s^- p$ candidates is shown in figure 3. A clear $\Lambda_b^0 \to D_s^- p$ signal peak is visible, corresponding to a yield of $831 \pm 32$, where the uncertainty is statistical. This result constitutes the first observation of this decay. A few bins around $5575\,\mathrm{MeV}/c^2$ show a disagreement between the model and the data. This has been scrutinised and any possible effect of this is expected to be covered by systematic uncertainties. This includes the systematic uncertainties on the shape and yield of the misidentified background components, as discussed in section 5. Additionally, the fraction between the two functions used for the shape of the $\Lambda_b^0 \to D_s^{*-} p$ contribution has been allowed to vary, which has a negligible effect on the signal yield.

The fits to $\Lambda_b^0 \to D_s^- p$ and $\Lambda_b^0 \to \Lambda_c^+ \pi^-$ candidates are studied for stability and any bias on the signal yields using pseudoexperiments. The fits are found to be stable, and no sizeable biases have been found. Furthermore, the fit is validated using data split according to magnet polarity, year of data taking, BDTG response and trigger decision.

## 5  Systematic uncertainties

Systematic uncertainties arising from the limited knowledge of the background and signal shapes, the expected background yields and the PID and hardware trigger efficiencies are considered. Due to similarities between the $\Lambda_b^0 \to D_s^- p$ and the $\Lambda_b^0 \to \Lambda_c^+ \pi^-$ decay topologies, many sources of systematic uncertainties either cancel or are suppressed. The remaining systematic uncertainties are outlined below and summarised in table 2.

Systematic uncertainties are assigned to the determination of the $\Lambda_b^0 \to D_s^- p$ and $\Lambda_b^0 \to \Lambda_c^+ \pi^-$ yields, which are obtained from invariant-mass fits. These uncertainties are determined using ensembles of pseudoexperiments comparing the results from alternative fit configurations.

For the parametrisation of the signal, the fixed parameters are varied within their uncertainties leading to a variation of 0.54% and 0.27% in the $\Lambda_b^0 \to D_s^- p$ and $\Lambda_b^0 \to \Lambda_c^+ \pi^-$ yields, respectively. Systematic uncertainties on the combinatorial background are assessed using pseudoexperiments with alternative parametrisations. In the fit to $\Lambda_b^0 \to D_s^- p$
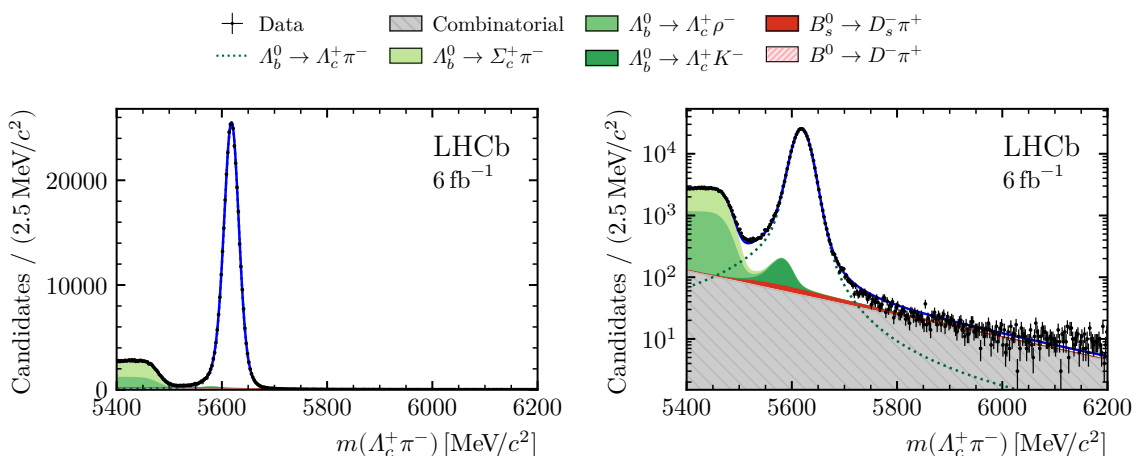
**Figure 2**. Invariant-mass distribution of $\Lambda_b^0 \to \Lambda_c^+ \pi^-$ candidates, the normalisation channel in this measurement. The size of the signal peak compared to the backgrounds can be seen clearly in the linear plot on the left, whereas the individual components are displayed more clearly in the logarithmic plot on the right. Overlaid are the fit projections of the signal and background contributions, with individual components illustrated in the legend above.
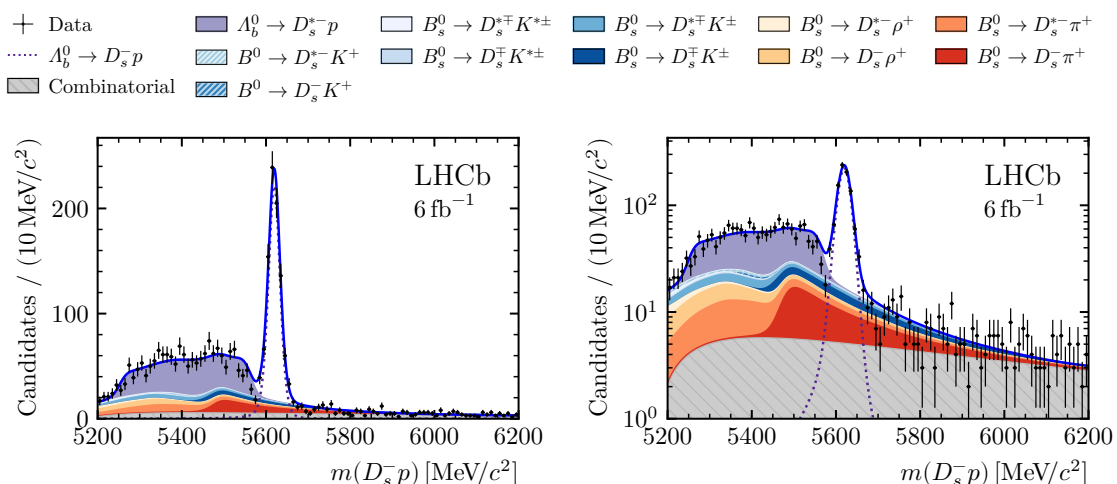


**Figure 3**. Invariant-mass distribution of $\Lambda_b^0 \to D_s^- p$ candidates, in (left) linear and (right) logarithmic scale, where the fit projections of the signal and background contributions are overlaid. The individual components in the fit are illustrated in the legend. A few bins around $5575\,\mathrm{MeV}/c^2$ show a disagreement between the model and the data. This effect is covered by the systematic uncertainties as described in the text.

candidates, an exponential function is chosen as an alternative to the parametrisation described in the previous section. The observed variation of 0.73% is assigned as a systematic uncertainty. A single exponential describes the combinatorial background in the nominal $m(\Lambda_c^+ \pi^-)$ fit. In contrast, the sum of two exponential functions is used to assign systematic uncertainties. This uncertainty amounts to only 0.04% on the final result.

The yields of the misidentified background components in the default invariant-mass fits are constrained or fixed. The corresponding systematic uncertainty in this assumption is calculated by varying their central values by 10%, which is twice the uncertainty on the calculated values, to conservatively take into account any bias in the procedure. This results in a systematic uncertainty of 0.71% and 0.03% in the $m(D_s^- p)$ and $m(\Lambda_c^+ \pi^-)$ fits, respectively.

All the shapes of the misidentified and partially reconstructed background components are varied by applying the PID calibration as a function of different variables. Samples of $D^{*+} \to D^0 \pi^+$ and $\Lambda_c^+ \to pK^-\pi^+$ calibration data are used to obtain weighting histograms. In the default calibration procedure, these histograms depend on the pseudorapidity and momentum of a track. For systematic studies, they are binned as a function of the number of tracks in the event and the candidate track momentum. This variation results in a systematic uncertainty of 0.89% in the sample of $\Lambda_b^0 \to D_s^- p$ candidates and a negligible 0.01% for the $\Lambda_b^0 \to \Lambda_c^+ \pi^-$ candidates. Together, the systematic uncertainties on the fit model amount to 1.46% and 0.28% for the fit to $\Lambda_b^0 \to D_s^- p$ and $\Lambda_b^0 \to \Lambda_c^+ \pi^-$ candidates, respectively.

A systematic uncertainty on the PID selection efficiency is determined by changing the binning scheme of the PID weighting histograms. By reducing and increasing the number of bins, the efficiency ratio $\epsilon(\Lambda_b^0 \to \Lambda_c^+ \pi^-)/\epsilon(\Lambda_b^0 \to D_s^- p)$ changes by 0.49%, which is therefore assigned as a systematic uncertainty on the final result. This uncertainty mainly originates from the tight PID requirement on the companion proton of the $\Lambda_b^0 \to D_s^- p$ signal.

The efficiency of the hardware trigger requirements is estimated from $D^{*+}$ and $\Lambda^0$ calibration samples and using simulation of signal candidates, using a similar method to the one described in ref. [38]. The difference between data and simulation amounts to 1.15% and is assigned as a systematic uncertainty on the branching fraction result.

Finally, a systematic uncertainty of 0.50% is assigned to the reconstruction efficiency of the charged hadron tracks. This is mainly due to the uncertainty in simulating the LHCb material correctly and the pion-kaon difference in the final-state particles of the signal and normalisation channels, which have a different interaction cross-section with the material [39].

In summary, the systematic uncertainties in this measurement amount to 2.01% on the final branching fraction result. This uncertainty is smaller than the statistical uncertainty and the uncertainties arising from the branching fraction inputs.

## 6 Results and conclusions

The branching fraction of $\Lambda_b^0 \to D_s^- p$ can be determined using the efficiencies of the requirements detailed in section 3 and the yields of the $\Lambda_b^0 \to D_s^- p$ and $\Lambda_b^0 \to \Lambda_c^+ \pi^-$ decays as obtained in section 4. Additionally, inputs for the $\Lambda_b^0 \to \Lambda_c^+ \pi^-$, $\Lambda_c^+ \to pK^-\pi^+$ and $D_s^- \to K^-K^+\pi^-$ branching fractions are required, as defined in eq. (1.2). Table 3 shows a summary of the inputs necessary for this measurement.

| Source | Relative uncertainty (%) |
|---|---|
| Invariant-mass fits: | |
| $\quad m(D_s^- p)$ fit: | |
| $\qquad$ Signal parametrisation | 0.54 |
| $\qquad$ Combinatorial background parametrisation | 0.73 |
| $\qquad$ Constrained/fixed yields | 0.71 |
| $\qquad$ Specific background parametrisation | 0.89 |
| $\quad m(\Lambda_c^+ \pi^-)$ fit: | |
| $\qquad$ Signal parametrisation | 0.27 |
| $\qquad$ Combinatorial background parametrisation | 0.04 |
| $\qquad$ Constrained/fixed yields | 0.03 |
| $\qquad$ Specific background parametrisation | 0.01 |
| Efficiencies: | |
| $\quad$ PID efficiency | 0.49 |
| $\quad$ hardware trigger efficiency | 1.15 |
| $\quad$ Reconstruction efficiency | 0.50 |
| Total | 2.01 |

**Table 2**. Summary of the systematic uncertainties as a percentage of the branching fraction of the $\Lambda_b^0 \to D_s^- p$ decay. The total systematic uncertainty is the quadratic sum of the individual sources.

| | $\Lambda_b^0 \to D_s^- p$ | $\Lambda_b^0 \to \Lambda_c^+ \pi^-$ |
|---|---|---|
| Yield | $831 \pm 32$ | $(4.047 \pm 0.007) \times 10^5$ |
| Efficiency | $(0.1819 \pm 0.0013)\%$ | $(0.1947 \pm 0.0012)\%$ |
| $\mathcal{B}(\Lambda_b^0 \to \Lambda_c^+ \pi^-)$ | $(4.9\ \pm 0.4\ ) \times 10^{-3}$ | [7] |
| $\mathcal{B}(D_s^- \to K^- K^+ \pi^-)$ | $(5.38 \pm 0.10) \times 10^{-2}$ | [7] |
| $\mathcal{B}(\Lambda_c^+ \to p K^- \pi^+)$ | $(6.28 \pm 0.32) \times 10^{-2}$ | [7] |

**Table 3**. Obtained signal yields and efficiencies of the $\Lambda_b^0 \to D_s^- p$ and $\Lambda_b^0 \to \Lambda_c^+ \pi^-$ decays, as well as branching fractions used for this measurement [7]. The uncertainty on the signal yields and efficiencies is statistical.

The branching-fraction ratio of the $\Lambda_b^0 \to D_s^- p$ and $\Lambda_b^0 \to \Lambda_c^+ \pi^-$ decays is found to be

$$\frac{\mathcal{B}(\Lambda_b^0 \to D_s^- p)}{\mathcal{B}(\Lambda_b^0 \to \Lambda_c^+ \pi^-)} = (2.56 \pm 0.10 \pm 0.05 \pm 0.14) \times 10^{-3} \,,$$

where the first uncertainty is statistical, the second systematic and the third due to the uncertainty of the $D_s^- \to K^- K^+ \pi^-$ and $\Lambda_c^+ \to p K^- \pi^+$ branching fractions.

The obtained $\Lambda_b^0 \to D_s^- p$ branching fraction is

$$\mathcal{B}(\Lambda_b^0 \to D_s^- p) = (12.6 \pm 0.5 \pm 0.3 \pm 1.2) \times 10^{-6} \,,$$

where the third uncertainty is due to the uncertainty of the $\Lambda_b^0 \to \Lambda_c^+ \pi^-$, $D_s^- \to K^- K^+ \pi^-$ and $\Lambda_c^+ \to p K^- \pi^+$ branching fractions. This measurement is limited by the uncertainty on the $\Lambda_b^0 \to \Lambda_c^+ \pi^-$ branching fraction, which is dominated by the precision on the ratio of hadronisation fractions $f_{\Lambda_b^0}/f_d$.

In summary, the first observation of the $\Lambda_b^0 \to D_s^- p$ decay and its branching fraction measurement are reported. Additionally, the branching fraction ratio of the $\Lambda_b^0 \to D_s^- p$ and $\Lambda_b^0 \to \Lambda_c^+ \pi^-$ decays is determined. This measurement will serve as input for future studies of factorisation in hadronic $\Lambda_b^0$ decays.

## Acknowledgments

## A  Particle identification selection on the companion particle

Figure 4 shows invariant-mass distributions of $\Lambda_b^0 \to D_s^- p$ and $\Lambda_b^0 \to \Lambda_c^+ \pi^-$ candidates. The candidates are selected by applying the full offline selection without the particle identification (PID) requirement on the companion track. This is represented as the filled orange ($\Lambda_b^0 \to D_s^- p$) and green ($\Lambda_b^0 \to \Lambda_c^+ \pi^-$) histograms. Candidates additionally passing or failing the PID requirements on the companion track are indicated by circles and squares, respectively.

## B  Invariant-mass fits to the control channels

To estimate the contribution from $D_s^- \pi^+$-like decays in the $B_s^0 \to D_s^\mp K^\pm$ and $\Lambda_b^0 \to D_s^- p$ data samples, an invariant-mass fit to the $B_s^0 \to D_s^- \pi^+$, $D_s^- \to K^- K^+ \pi^-$ sample under its own hypothesis is performed. The invariant-mass distribution of the $B_s^0 \to D_s^- \pi^+$ candidates is shown in figure 5. The fit model is composed of a signal contribution described by the sum of a double-sided Hypatia function and a Johnson $S_U$ function, combinatorial background described by a single exponential and specific background components. Three different sources of specific background can be distinguished: the decays with the same final state as the signal ($B^0 \to D_s^- \pi^+$), the misidentified backgrounds ($B^0 \to D^- \pi^+$, $\Lambda_b^0 \to \Lambda_c^+ \pi^-$, $B_s^0 \to D_s^\mp K^\pm$) and the partially-reconstructed backgrounds which occur due to missing particles in the final state ($B^0 \to D_s^{*-} \pi^+$, $B_s^0 \to D_s^{*-} \pi^+$, $B_s^0 \to D_s^- \rho^+$, $B_s^0 \to D_s^{*-} \rho^+$). The
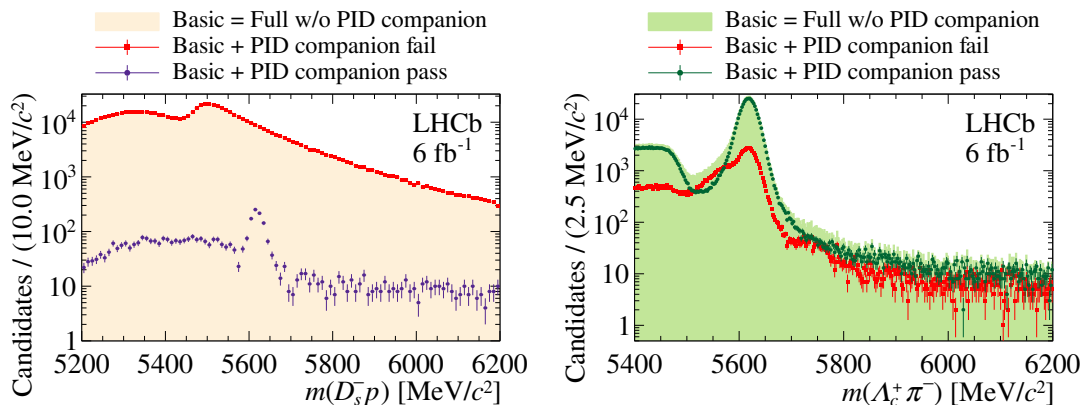
**Figure 4.** The (left) $m(D_s^- p)$ and (right) $m(\Lambda_c^+ \pi^-)$ invariant-mass distributions after the full selection without the PID requirement on the companion track (filled area) and passing (circles) or failing (squares) this selection.
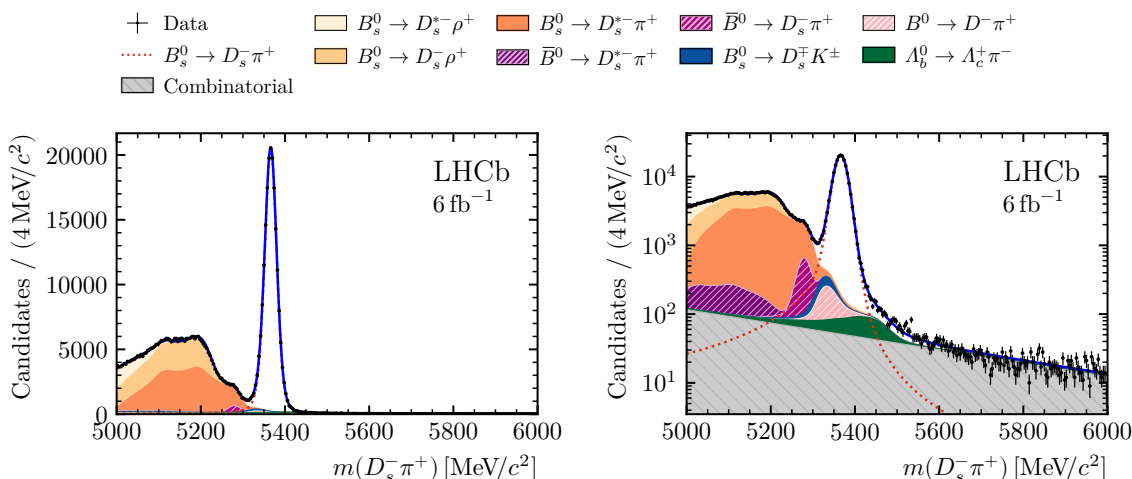


**Figure 5.** Invariant-mass distribution of $B_s^0 \to D_s^- \pi^+$ candidates, in (left) linear and (right) logarithmic scale, where the signal and background contributions are overlaid. The individual components of the fit are illustrated in the legend.

shapes of specific backgrounds are taken from the simulated samples. The expected yields of $B_s^0 \to D_s^\mp K^\pm$, $B^0 \to D^- \pi^+$ and $\Lambda_b^0 \to \Lambda_c^+ \pi^-$ decays are calculated from the branching fractions and efficiency predictions. They are found to be below 1% of the signal component and are fixed in the fit. In the default data fit, the signal mean and width, the combinatorial background slope and the yields are left free.

The contribution from the $D_s^\mp K^\pm$-like decays in the $\Lambda_b^0 \to D_s^- p$ data sample is estimated from an invariant-mass fit to the $B_s^0 \to D_s^\mp K^\pm$ sample under its own hypothesis. The invariant-mass distribution of the $B_s^0 \to D_s^\mp K^\pm$ candidates is shown in figure 6. The fit model is composed of a signal contribution described by the sum of a double-sided Hypatia function and a Johnson $S_U$ function, combinatorial background described by a single exponential and specific background components. Unlike in the $B_s^0 \to D_s^- \pi^+$ sample, four
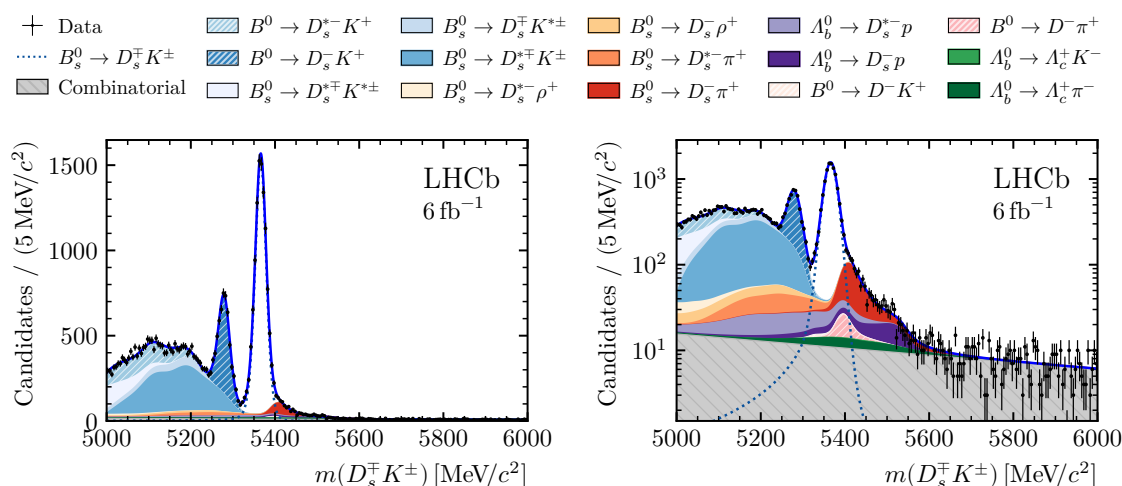
**Figure 6**. Invariant-mass distribution of $B_s^0 \to D_s^{\mp} K^{\pm}$ candidates, in (left) linear and (right) logarithmic scale, where the signal and background contributions are overlaid. The individual components in the fit are illustrated in the legend.

different sources of background for $B_s^0 \to D_s^{\mp} K^{\pm}$ signal can be distinguished: the decays with the same final state as the signal ($B^0 \to D_s^- K^+$), the partially-reconstructed backgrounds which occur due to missing particles in the final state ($B^0 \to D_s^{*-} K^+$, $B_s^0 \to D_s^{*\mp} K^{\pm}$, $B_s^0 \to D_s^{\mp} K^{*\pm}$, $B_s^0 \to D_s^{*\mp} K^{*\pm}$), the misidentified backgrounds ($B_s^0 \to D_s^- \pi^+$, $\Lambda_b^0 \to D_s^- p$) and the backgrounds that are both partially reconstructed and misidentified ($B_s^0 \to D_s^{*-} \pi^+$, $B_s^0 \to D_s^- \rho^+$, $B_s^0 \to D_s^{*-} \rho^+$, $\Lambda_b^0 \to D_s^{*-} p$). To improve the stability of the fit, the contributions from the suppressed $B_s^0 \to D_s^{(*)-} \{\pi^+, \rho^+\}$ decays are fixed using the fit to $B_s^0 \to D_s^- \pi^+$ candidates, while the remaining yields of the $B^0 \to D^- \pi^+$, $B^0 \to D^- K^+$, $\Lambda_b^0 \to \Lambda_c^+ \pi^-$ and $\Lambda_b^0 \to \Lambda_c^+ K^-$ decays are calculated from their branching fractions and relative efficiencies. In the default data fit, the signal mean and width, the combinatorial background slope and the yields are left free.

## References

[1] N. Cabibbo, *Unitary symmetry and leptonic decays*, *Phys. Rev. Lett.* **10** (1963) 531 [INSPIRE].

[2] M. Kobayashi and T. Maskawa, *CP violation in the renormalizable theory of weak interaction*, *Prog. Theor. Phys.* **49** (1973) 652 [INSPIRE].

[3] J. Charles et al., *Current status of the Standard Model CKM fit and constraints on $\Delta F = 2$ new physics*, *Phys. Rev. D* **91** (2015) 073007 [arXiv:1501.05013] [INSPIRE].

[4] UTFIT collaboration, *The unitarity triangle fit in the Standard Model and hadronic parameters from lattice QCD: a reappraisal after the measurements of $\Delta m_s$ and $BR(B \to \tau \nu_\tau)$*, *JHEP* **10** (2006) 081 [hep-ph/0606167] [INSPIRE].

[5] A. Bazavov et al., *B- and D-meson leptonic decay constants from four-flavor lattice QCD*, *Phys. Rev. D* **98** (2018) 074512 [arXiv:1712.09262] [INSPIRE].

[6] N. Carrasco et al., *Leptonic decay constants $f_K, f_D$, and $f_{D_s}$ with $N_f = 2 + 1 + 1$ twisted-mass lattice QCD*, *Phys. Rev. D* **91** (2015) 054507 [arXiv:1411.7908] [INSPIRE].

[7] PARTICLE DATA GROUP collaboration, *Review of particle physics*, *PTEP* **2022** (2022) 083C01 [INSPIRE].

[8] M. Beneke, G. Buchalla, M. Neubert and C.T. Sachrajda, *QCD factorization for exclusive, nonleptonic B meson decays: General arguments and the case of heavy light final states*, *Nucl. Phys. B* **591** (2000) 313 [hep-ph/0006124] [INSPIRE].

[9] LHCb collaboration, *Measurement of the branching fraction of the $B^0 \to D_s^+ \pi^-$ decay*, *Eur. Phys. J. C* **81** (2021) 314 [arXiv:2010.11986] [INSPIRE].

[10] P. Ball and R. Zwicky, *New results on $B \to \pi, K, \eta$ decay formfactors from light-cone sum rules*, *Phys. Rev. D* **71** (2005) 014015 [hep-ph/0406232] [INSPIRE].

[11] P. Ball, *|V(ub)| from UTangles and $B \to \pi \ell \nu$*, *Phys. Lett. B* **644** (2007) 38 [hep-ph/0611108] [INSPIRE].

[12] W. Detmold, C. Lehner and S. Meinel, *$\Lambda_b \to p \ell^- \bar{\nu}_\ell$ and $\Lambda_b \to \Lambda_c \ell^- \bar{\nu}_\ell$ form factors from lattice QCD with relativistic heavy quarks*, *Phys. Rev. D* **92** (2015) 034503 [arXiv:1503.01421] [INSPIRE].

[13] LHCb collaboration, *The LHCb detector at the LHC*, 2008 *JINST* **3** S08005 [INSPIRE].

[14] LHCb collaboration, *LHCb detector performance*, *Int. J. Mod. Phys. A* **30** (2015) 1530022 [arXiv:1412.6352] [INSPIRE].

[15] V.V. Gligorov and M. Williams, *Efficient, reliable and fast high-level triggering using a bonsai boosted decision tree*, 2013 *JINST* **8** P02013 [arXiv:1210.6861] [INSPIRE].

[16] T. Likhomanenko et al., *LHCb topological trigger reoptimization*, *J. Phys. Conf. Ser.* **664** (2015) 082025 [arXiv:1510.00572] [INSPIRE].

[17] T. Sjostrand, S. Mrenna and P.Z. Skands, *A brief introduction to PYTHIA 8.1*, *Comput. Phys. Commun.* **178** (2008) 852 [arXiv:0710.3820] [INSPIRE].

[18] I. Belyaev et al., *Handling of the generation of primary events in Gauss, the LHCb simulation framework*, *J. Phys. Conf. Ser.* **331** (2011) 032047 [INSPIRE].

[19] D.J. Lange, *The EvtGen particle decay simulation package*, *Nucl. Instrum. Meth. A* **462** (2001) 152 [INSPIRE].

[20] N. Davidson, T. Przedzinski and Z. Was, *PHOTOS interface in C++: technical and physics documentation*, *Comput. Phys. Commun.* **199** (2016) 86 [arXiv:1011.0937] [INSPIRE].

[21] J. Allison et al., *Geant4 developments and applications*, *IEEE Trans. Nucl. Sci.* **53** (2006) 270 [INSPIRE].

[22] GEANT4 collaboration, *GEANT4 — a simulation toolkit*, *Nucl. Instrum. Meth. A* **506** (2003) 250 [INSPIRE].

[23] M. Clemencic et al., *The LHCb simulation application, Gauss: Design, evolution and experience*, *J. Phys. Conf. Ser.* **331** (2011) 032023 [INSPIRE].

[24] W.D. Hulsbergen, *Decay chain fitting with a Kalman filter*, *Nucl. Instrum. Meth. A* **552** (2005) 566 [physics/0503191] [INSPIRE].

[25] L. Breiman, J.H. Friedman, R.A. Olshen and C.J. Stone, *Classification and regression trees*, Wadsworth international group, Belmont, California, U.S.A. (1984).

[26] B.P. Roe et al., *Boosted decision trees, an alternative to artificial neural networks*, *Nucl. Instrum. Meth. A* **543** (2005) 577 [physics/0408124] [INSPIRE].

[27] LHCb collaboration, *Measurement of CP asymmetry in $B_s^0 \to D_s^\mp K^\pm$ decays*, *JHEP* **03** (2018) 059 [arXiv:1712.07428] [INSPIRE].

[28] U.P. Eitschberger, *Flavour-tagged measurement of CP observables in $B_s^0 \to D_s^\mp K^\pm$ decays with the LHCb experiment*, Ph.D. thesis, Tech. U., Dortmund (2018) [INSPIRE].

[29] L. Anderlini et al., *PIDCalib package* LHCb-PUB-2016-021, CERN, Geneva (2016).

[30] G. Punzi, *Sensitivity of searches for new signals and its optimization*, *eConf* **C030908** (2003) MODT002 [physics/0308063] [INSPIRE].

[31] R. Aaij et al., *Selection and processing of calibration samples to measure the particle identification performance of the LHCb experiment in Run 2*, *EPJ Tech. Instrum.* **6** (2019) 1 [arXiv:1803.00824] [INSPIRE].

[32] D. Martínez Santos and F. Dupertuis, *Mass distributions marginalized over per-event errors*, *Nucl. Instrum. Meth. A* **764** (2014) 150 [arXiv:1312.5000] [INSPIRE].

[33] N.L. Johnson, *Systems of frequency curves generated by methods of translation*, *Biometrika* **36** (1949) 149 [INSPIRE].

[34] LHCb collaboration, *Measurement of CP observables in $B^\pm \to D^{(*)}K^\pm$ and $B^\pm \to D^{(*)}\pi^\pm$ decays*, *Phys. Lett. B* **777** (2018) 16 [arXiv:1708.06370] [INSPIRE].

[35] K.S. Cranmer, *Kernel estimation in high-energy physics*, *Comput. Phys. Commun.* **136** (2001) 198 [hep-ex/0011057] [INSPIRE].

[36] T. Skwarnicki, *A study of the radiative CASCADE transitions between the Upsilon-Prime and Upsilon resonances*, Ph.D. thesis, Krakow, INP, Poland (1986) [INSPIRE].

[37] LHCb collaboration, *Studies of beauty baryon decays to $D^0 p h^-$ and $\Lambda_c^+ h^-$ final states*, *Phys. Rev. D* **89** (2014) 032001 [arXiv:1311.4823] [INSPIRE].

[38] LHCb collaboration, *Observation of the decay $B_s^0 \to \overline{D}^0 K^+ K^-$*, *Phys. Rev. D* **98** (2018) 072006 [arXiv:1807.01891] [INSPIRE].

[39] LHCb collaboration, *Measurement of the branching fraction and CP asymmetry in $B^+ \to J/\psi \rho^+$ decays*, *Eur. Phys. J. C* **79** (2019) 537 [arXiv:1812.07041] [INSPIRE].

# The LHCb collaboration

R. Aaij [ID][32], A.S.W. Abdelmotteleb [ID][50], C. Abellan Beteta[44], F. Abudinén [ID][50], T. Ackernley [ID][54],
B. Adeva [ID][40], M. Adinolfi [ID][48], P. Adlarson [ID][77], H. Afsharnia[9], C. Agapopoulou [ID][13],
C.A. Aidala [ID][78], Z. Ajaltouni[9], S. Akar [ID][59], K. Akiba [ID][32], P. Albicocco [ID][23], J. Albrecht [ID][15],
F. Alessio [ID][42], M. Alexander [ID][53], A. Alfonso Albero [ID][39], Z. Aliouche [ID][56], P. Alvarez Cartelle [ID][49],
R. Amalric [ID][13], S. Amato [ID][2], J.L. Amey [ID][48], Y. Amhis [ID][11,42], L. An [ID][42], L. Anderlini [ID][22],
M. Andersson [ID][44], A. Andreianov [ID][38], M. Andreotti [ID][21], D. Andreou [ID][62], D. Ao [ID][6],
F. Archilli [ID][31,t], A. Artamonov [ID][38], M. Artuso [ID][62], E. Aslanides [ID][10], M. Atzeni [ID][44],
B. Audurier [ID][12], I.B Bachiller Perea [ID][8], S. Bachmann [ID][17], M. Bachmayer [ID][43], J.J. Back [ID][50],
A. Bailly-reyre[13], P. Baladron Rodriguez [ID][40], V. Balagura [ID][12], W. Baldini [ID][21,42],
J. Baptista de Souza Leite [ID][1], M. Barbetti [ID][22,j], R.J. Barlow [ID][56], S. Barsuk [ID][11], W. Barter [ID][52],
M. Bartolini [ID][49], F. Baryshnikov [ID][38], J.M. Basels [ID][14], G. Bassi [ID][29,q], B. Batsukh [ID][4],
A. Battig [ID][15], A. Bay [ID][43], A. Beck [ID][50], M. Becker [ID][15], F. Bedeschi [ID][29], I.B. Bediaga [ID][1],
A. Beiter[62], S. Belin [ID][40], V. Bellee [ID][44], K. Belous [ID][38], I. Belov [ID][38], I. Belyaev [ID][38], G. Benane [ID][10],
G. Bencivenni [ID][23], E. Ben-Haim [ID][13], A. Berezhnoy [ID][38], R. Bernet [ID][44], S. Bernet Andres [ID][76],
D. Berninghoff[17], H.C. Bernstein[62], C. Bertella [ID][56], A. Bertolin [ID][28], C. Betancourt [ID][44],
F. Betti [ID][42], Ia. Bezshyiko [ID][44], S. Bhasin [ID][48], J. Bhom [ID][35], L. Bian [ID][68], M.S. Bieker [ID][15],
N.V. Biesuz [ID][21], P. Billoir [ID][13], A. Biolchini [ID][32], M. Birch [ID][55], F.C.R. Bishop [ID][49], A. Bitadze [ID][56],
A. Bizzeti [ID], M.P. Blago [ID][49], T. Blake [ID][50], F. Blanc [ID][43], J.E. Blank [ID][15], S. Blusk [ID][62],
D. Bobulska [ID][53], J.A. Boelhauve [ID][15], O. Boente Garcia [ID][12], T. Boettcher [ID][59], A. Boldyrev [ID][38],
C.S. Bolognani [ID][74], R. Bolzonella [ID][21,i], N. Bondar [ID][38,42], F. Borgato [ID][28], S. Borghi [ID][56],
M. Borsato [ID][17], J.T. Borsuk [ID][35], S.A. Bouchiba [ID][43], T.J.V. Bowcock [ID][54], A. Boyer [ID][42],
C. Bozzi [ID][21], M.J. Bradley[55], S. Braun [ID][60], A. Brea Rodriguez [ID][40], J. Brodzicka [ID][35],
A. Brossa Gonzalo [ID][40], J. Brown [ID][54], D. Brundu [ID][27], A. Buonaura [ID][44], L. Buonincontri [ID][28],
A.T. Burke [ID][56], C. Burr [ID][42], A. Bursche[66], A. Butkevich [ID][38], J.S. Butter [ID][32], J. Buytaert [ID][42],
W. Byczynski [ID][42], S. Cadeddu [ID][27], H. Cai[68], R. Calabrese [ID][21,i], L. Calefice [ID][15], S. Cali [ID][23],
M. Calvi [ID][26,m], M. Calvo Gomez [ID][76], P. Campana [ID][23], D.H. Campora Perez [ID][74],
A.F. Campoverde Quezada [ID][6], S. Capelli [ID][26,m], L. Capriotti [ID][20], A. Carbone [ID][20,g],
R. Cardinale [ID][24,k], A. Cardini [ID][27], P. Carniti [ID][26,m], L. Carus[14], A. Casais Vidal [ID][40],
R. Caspary [ID][17], G. Casse [ID][54], M. Cattaneo [ID][42], G. Cavallero [ID][55,42], V. Cavallini [ID][21,i],
S. Celani [ID][43], J. Cerasoli [ID][10], D. Cervenkov [ID][57], A.J. Chadwick [ID][54], I. Chahrour [ID][78],
M.G. Chapman[48], M. Charles [ID][13], Ph. Charpentier [ID][42], C.A. Chavez Barajas [ID][54],
M. Chefdeville [ID][8], C. Chen [ID][10], S. Chen [ID][4], A. Chernov [ID][35], S. Chernyshenko [ID][46],
V. Chobanova [ID][40], S. Cholak [ID][43], M. Chrzaszcz [ID][35], A. Chubykin [ID][38], V. Chulikov [ID][38],
P. Ciambrone [ID][23], M.F. Cicala [ID][50], X. Cid Vidal [ID][40], G. Ciezarek [ID][42], P. Cifra [ID][42], G. Ciullo [ID][i,21],
P.E.L. Clarke [ID][52], M. Clemencic [ID][42], H.V. Cliff [ID][49], J. Closier [ID][42], J.L. Cobbledick [ID][56],
V. Coco [ID][42], J.A.B. Coelho [ID][11], J. Cogan [ID][10], E. Cogneras [ID][9], L. Cojocariu [ID][37], P. Collins [ID][42],
T. Colombo [ID][42], L. Congedo [ID][19], A. Contu [ID][27], N. Cooke [ID][47], I. Corredoira [ID][40], G. Corti [ID][42],
B. Couturier [ID][42], D.C. Craik [ID][44], M. Cruz Torres [ID][1,e], R. Currie [ID][52], C.L. Da Silva [ID][61],
S. Dadabaev [ID][38], L. Dai [ID][65], X. Dai [ID][5], E. Dall'Occo [ID][15], J. Dalseno [ID][40], C. D'Ambrosio [ID][42],
J. Daniel [ID][9], A. Danilina [ID][38], P. d'Argent [ID][19], J.E. Davies [ID][56], A. Davis [ID][56],
O. De Aguiar Francisco [ID][56], J. de Boer [ID][42], K. De Bruyn [ID][73], S. De Capua [ID][56], M. De Cian [ID][43],

U. De Freitas Carneiro Da Graca [1], E. De Lucia [23], J.M. De Miranda [1], L. De Paula[2],
M. De Serio [19,f], D. De Simone [44], P. De Simone [23], F. De Vellis [15], J.A. de Vries [74],
C.T. Dean [61], F. Debernardis [19,f], D. Decamp [8], V. Dedu [10], L. Del Buono [13],
B. Delaney [58], H.-P. Dembinski [15], V. Denysenko [44], O. Deschamps [9], F. Dettori [27,h],
B. Dey [71], P. Di Nezza [23], I. Diachkov [38], S. Didenko [38], L. Dieste Maronas[40], S. Ding [62],
V. Dobishuk [46], A. Dolmatov[38], C. Dong [3], A.M. Donohoe [18], F. Dordei [27], A.C. dos Reis [1],
L. Douglas[53], A.G. Downes [8], P. Duda [75], M.W. Dudek [35], L. Dufour [42], V. Duk [72],
P. Durante [42], M. M. Duras [75], J.M. Durham [61], D. Dutta [56], A. Dziurda [35],
A. Dzyuba [38], S. Easo [51], U. Egede [63], V. Egorychev [38], C. Eirea Orro[40], S. Eisenhardt [52],
E. Ejopu [56], S. Ek-In [43], L. Eklund [77], J. Ellbracht [15], S. Ely [55], A. Ene [37], E. Epple [59],
S. Escher [14], J. Eschle [44], S. Esen [44], T. Evans [56], F. Fabiano [27,h], L.N. Falcao [1],
Y. Fan [6], B. Fang [11,68], L. Fantini [72,p], M. Faria [43], S. Farry [54], D. Fazzini [26,m],
L.F Felkowski [75], M. Feo [42], M. Fernandez Gomez [40], A.D. Fernez [60], F. Ferrari [20],
L. Ferreira Lopes [43], F. Ferreira Rodrigues [2], S. Ferreres Sole [32], M. Ferrillo [44],
M. Ferro-Luzzi [42], S. Filippov [38], R.A. Fini [19], M. Fiorini [21,i], M. Firlej [34],
K.M. Fischer [57], D.S. Fitzgerald [78], C. Fitzpatrick [56], T. Fiutowski [34], F. Fleuret [12],
M. Fontana [13], F. Fontanelli [24,k], R. Forty [42], D. Foulds-Holt [49], V. Franco Lima [54],
M. Franco Sevilla [60], M. Frank [42], E. Franzoso [21,i], G. Frau [17], C. Frei [42], D.A. Friday [53],
L. Frontini [25], J. Fu [6], Q. Fuehring [15], T. Fulghesu [13], E. Gabriel [32], G. Galati [19,f],
M.D. Galati [32], A. Gallas Torreira [40], D. Galli [20,g], S. Gambetta [52,42], M. Gandelman [2],
P. Gandini [25], Y. Gao [7], Y. Gao [5], M. Garau [27,h], L.M. Garcia Martin [50],
P. Garcia Moreno [39], J. García Pardiñas [26,m], B. Garcia Plana[40], F.A. Garcia Rosales [12],
L. Garrido [39], C. Gaspar [42], R.E. Geertsema [32], D. Gerick[17], L.L. Gerken [15],
E. Gersabeck [56], M. Gersabeck [56], T. Gershon [50], L. Giambastiani [28], V. Gibson [49],
H.K. Giemza [36], A.L. Gilman [57], M. Giovannetti [23,t], A. Gioventù [40],
P. Gironella Gironell [39], C. Giugliano [21,i], M.A. Giza [35], K. Gizdov [52], E.L. Gkougkousis [42],
V.V. Gligorov [13,42], C. Göbel [64], E. Golobardes [76], D. Golubkov [38], A. Golutvin [55,38],
A. Gomes [1,a], S. Gomez Fernandez [39], F. Goncalves Abrantes [57], M. Goncerz [35], G. Gong [3],
I.V. Gorelov [38], C. Gotti [26], J.P. Grabowski [70], T. Grammatico [13],
L.A. Granado Cardoso [42], E. Graugés [39], E. Graverini [43], G. Graziani [], A. T. Grecu [37],
L.M. Greeven [32], N.A. Grieser [59], L. Grillo [53], S. Gromov [38], B.R. Gruberg Cazon [57], C.
Gu [3], M. Guarise [21,i], M. Guittiere [11], P. A. Günther [17], E. Gushchin [38], A. Guth[14],
Y. Guz [38], T. Gys [42], T. Hadavizadeh [63], C. Hadjivasiliou [60], G. Haefeli [43], C. Haen [42],
J. Haimberger [42], S.C. Haines [49], T. Halewood-leagas [54], M.M. Halvorsen [42],
P.M. Hamilton [60], J. Hammerich [54], Q. Han [7], X. Han [17], E.B. Hansen [56],
S. Hansmann-Menzemer [17], L. Hao [6], N. Harnew [57], T. Harrison [54], C. Hasse [42],
M. Hatch [42], J. He [6,c], K. Heijhoff [32], F.H Hemmer [42], C. Henderson [59],
R.D.L. Henderson [63,50], A.M. Hennequin [58], K. Hennessy [54], L. Henry [42], J. Herd [55],
J. Heuel [14], A. Hicheur [2], D. Hill [43], M. Hilton [56], S.E. Hollitt [15], J. Horswill [56],
R. Hou [7], Y. Hou [8], J. Hu[17], J. Hu [66], W. Hu [5], X. Hu [3], W. Huang [6], X. Huang[68],
W. Hulsbergen [32], R.J. Hunter [50], M. Hushchyn [38], D. Hutchcroft [54], P. Ibis [15],
M. Idzik [34], D. Ilin [38], P. Ilten [59], A. Inglessi [38], A. Iniukhin [38], A. Ishteev [38],
K. Ivshin [38], R. Jacobsson [42], H. Jage [14], S.J. Jaimes Elles [41], S. Jakobsen [42], E. Jans [32],

B.K. Jashal [41], A. Jawahery [60], V. Jevtic [15], E. Jiang [60], X. Jiang [4,6], Y. Jiang [6],
M. John [57], D. Johnson [58], C.R. Jones [49], T.P. Jones [50], B. Jost [42], N. Jurik [42],
I. Juszczak [35], S. Kandybei [45], Y. Kang [3], M. Karacson [42], D. Karpenkov [38],
M. Karpov [38], J.W. Kautz [59], F. Keizer [42], D.M. Keller [62], M. Kenzie [50], T. Ketel [32],
B. Khanji [15], A. Kharisova [38], S. Kholodenko [38], G. Khreich [11], T. Kirn [14],
V.S. Kirsebom [43], O. Kitouni [58], S. Klaver [33], N. Kleijne [29,q], K. Klimaszewski [36],
M.R. Kmiec [36], S. Koliiev [46], L. Kolk [15], A. Kondybayeva [38], A. Konoplyannikov [38],
P. Kopciewicz [34], R. Kopecna [17], P. Koppenburg [32], M. Korolev [38], I. Kostiuk [32,46], O. Kot [46],
S. Kotriakhova [], A. Kozachuk [38], P. Kravchenko [38], L. Kravchuk [38], R.D. Krawczyk [42],
M. Kreps [50], S. Kretzschmar [14], P. Krokovny [38], W. Krupa [34], W. Krzemien [36], J. Kubat [17],
S. Kubis [75], W. Kucewicz [35], M. Kucharczyk [35], V. Kudryavtsev [38], E.K Kulikova [38],
A. Kupsc [77], D. Lacarrere [42], G. Lafferty [56], A. Lai [27], A. Lampis [27,h], D. Lancierini [44],
C. Landesa Gomez [40], J.J. Lane [56], R. Lane [48], C. Langenbruch [14], J. Langer [15],
O. Lantwin [38], T. Latham [50], F. Lazzari [29,r], M. Lazzaroni [25,l], R. Le Gac [10], S.H. Lee [78],
R. Lefèvre [9], A. Leflat [38], S. Legotin [38], P. Lenisa [i,21], O. Leroy [10], T. Lesiak [35],
B. Leverington [17], A. Li [3], H. Li [66], K. Li [7], P. Li [42], P.-R. Li [67], S. Li [7], T. Li [4],
T. Li [66], Y. Li [4], Z. Li [62], X. Liang [62], C. Lin [6], T. Lin [51], R. Lindner [42],
V. Lisovskyi [15], R. Litvinov [27,h], G. Liu [66], H. Liu [6], Q. Liu [6], S. Liu [4,6],
A. Lobo Salvia [39], A. Loi [27], R. Lollini [72], J. Lomba Castro [40], I. Longstaff [53], J.H. Lopes [2],
A. Lopez Huertas [39], S. López Soliño [40], G.H. Lovell [49], Y. Lu [4,b], C. Lucarelli [22,j],
D. Lucchesi [28,o], S. Luchuk [38], M. Lucio Martinez [74], V. Lukashenko [32,46], Y. Luo [3],
A. Lupato [56], E. Luppi [21,i], A. Lusiani [29,q], K. Lynch [18], X.-R. Lyu [6], R. Ma [6],
S. Maccolini [15], F. Machefert [11], F. Maciuc [37], I. Mackay [57], V. Macko [43],
L.R. Madhan Mohan [48], A. Maevskiy [38], D. Maisuzenko [38], M.W. Majewski [34],
J.J. Malczewski [35], S. Malde [57], B. Malecki [35,42], A. Malinin [38], T. Maltsev [38],
G. Manca [27,h], G. Mancinelli [10], C. Mancuso [11,25,l], R. Manera Escalero [39], D. Manuzzi [20],
C.A. Manzari [44], D. Marangotto [25,l], J.F. Marchand [8], U. Marconi [20], S. Mariani [22,j],
C. Marin Benito [39], J. Marks [17], A.M. Marshall [48], P.J. Marshall [54], G. Martelli [72,p],
G. Martellotti [30], L. Martinazzoli [42,m], M. Martinelli [26,m], D. Martinez Santos [40],
F. Martinez Vidal [41], A. Massafferri [1], M. Materok [14], R. Matev [42], A. Mathad [44],
V. Matiunin [38], C. Matteuzzi [26], K.R. Mattioli [12], A. Mauri [32], E. Maurice [12],
J. Mauricio [39], M. Mazurek [42], M. McCann [55], L. Mcconnell [18], T.H. McGrath [56],
N.T. McHugh [53], A. McNab [56], R. McNulty [18], J.V. Mead [54], B. Meadows [59], G. Meier [15],
D. Melnychuk [36], S. Meloni [26,m], M. Merk [32,74], A. Merli [25,l], L. Meyer Garcia [2],
D. Miao [4,6], M. Mikhasenko [70,d], D.A. Milanes [69], E. Millard [50], M. Milovanovic [42],
M.-N. Minard [8,†], A. Minotti [26,m], T. Miralles [9], S.E. Mitchell [52], B. Mitreska [15],
D.S. Mitzel [15], A. Mödden [15], R.A. Mohammed [57], R.D. Moise [14], S. Mokhnenko [38],
T. Mombächer [40], M. Monk [50,63], I.A. Monroy [69], S. Monteil [9], G. Morello [23],
M.J. Morello [29,q], M.P. Morgenthaler [17], J. Moron [34], A.B. Morris [42], A.G. Morris [50],
R. Mountain [62], H. Mu [3], E. Muhammad [50], F. Muheim [52], M. Mulder [73], K. Müller [44],
C.H. Murphy [57], D. Murray [56], R. Murta [55], P. Muzzetto [27,h], P. Naik [48], T. Nakada [43],
R. Nandakumar [51], T. Nanut [42], I. Nasteva [2], M. Needham [52], N. Neri [25,l], S. Neubert [70],
N. Neufeld [42], P. Neustroev [38], R. Newcombe [55], J. Nicolini [15,11], D. Nicotra [74], E.M. Niel [43],

S. Nieswand[14], N. Nikitin [38], N.S. Nolte [58], C. Normand [8,h,27], J. Novoa Fernandez [40],
G.N Nowak [59], C. Nunez [78], A. Oblakowska-Mucha [34], V. Obraztsov [38], T. Oeser [14],
S. Okamura [21,i], R. Oldeman [27,h], F. Oliva [52], C.J.G. Onderwater [73], R.H. O'Neil [52],
J.M. Otalora Goicochea [2], T. Ovsiannikova [38], P. Owen [44], A. Oyanguren [41], O. Ozcelik [52],
K.O. Padeken [70], B. Pagare [50], P.R. Pais [42], T. Pajero [57], A. Palano [19], M. Palutan [23],
Y. Pan [56], G. Panshin [38], L. Paolucci [50], A. Papanestis [51], M. Pappagallo [19,f],
L.L. Pappalardo [21,i], C. Pappenheimer [59], W. Parker [60], C. Parkes [56], B. Passalacqua [21,i],
G. Passaleva [22], A. Pastore [19], M. Patel [55], C. Patrignani [20,g], C.J. Pawley [74],
A. Pellegrino [32], M. Pepe Altarelli [42], S. Perazzini [20], D. Pereima [38], A. Pereiro Castro [40],
P. Perret [9], K. Petridis [48], A. Petrolini [24,k], A. Petrov[38], S. Petrucci [52], M. Petruzzo [25],
H. Pham [62], A. Philippov [38], R. Piandani [6], L. Pica [29,q], M. Piccini [72], B. Pietrzyk [8],
G. Pietrzyk [11], M. Pili [57], D. Pinci [30], F. Pisani [42], M. Pizzichemi [26,m,42], V. Placinta [37],
J. Plews [47], M. Plo Casasus [40], F. Polci [13,42], M. Poli Lener [23], A. Poluektov [10],
N. Polukhina [38], I. Polyakov [42], E. Polycarpo [2], S. Ponce [42], D. Popov [6,42], S. Poslavskii [38],
K. Prasanth [35], L. Promberger [17], C. Prouve [40], V. Pugatch [46], V. Puill [11], G. Punzi [29,r],
H.R. Qi [3], W. Qian [6], N. Qin [3], S. Qu [3], R. Quagliani [43], N.V. Raab [18], B. Rachwal [34],
J.H. Rademacker [48], R. Rajagopalan[62], M. Rama [29], M. Ramos Pernas [50], M.S. Rangel [2],
F. Ratnikov [38], G. Raven [33,42], M. Rebollo De Miguel [41], F. Redi [42], J. Reich [48],
F. Reiss [56], C. Remon Alepuz[41], Z. Ren [3], P.K. Resmi [57], R. Ribatti [29,q], A.M. Ricci [27],
S. Ricciardi [51], K. Richardson [58], M. Richardson-Slipper [52], K. Rinnert [54], P. Robbe [11],
G. Robertson [52], A.B. Rodrigues [43], E. Rodrigues [54], E. Rodriguez Fernandez [40],
J.A. Rodriguez Lopez [69], E. Rodriguez Rodriguez [40], D.L. Rolf [42], A. Rollings [57],
P. Roloff [42], V. Romanovskiy [38], M. Romero Lamas [40], A. Romero Vidal [40], J.D. Roth[78,†],
M. Rotondo [23], M.S. Rudolph [62], T. Ruf [42], R.A. Ruiz Fernandez [40], J. Ruiz Vidal[41],
A. Ryzhikov [38], J. Ryzka [34], J.J. Saborido Silva [40], N. Sagidova [38], N. Sahoo [47],
B. Saitta [27,h], M. Salomoni [42], C. Sanchez Gras [32], I. Sanderswood [41], R. Santacesaria [30],
C. Santamarina Rios [40], M. Santimaria [23], E. Santovetti [31,t], D. Saranin [38], G. Sarpis [14],
M. Sarpis [70], A. Sarti [30], C. Satriano [30,s], A. Satta [31], M. Saur [15], D. Savrina [38],
H. Sazak [9], L.G. Scantlebury Smead [57], A. Scarabotto [13], S. Schael [14], S. Scherl [54],
M. Schiller [53], H. Schindler [42], M. Schmelling [16], B. Schmidt [42], S. Schmitt [14],
O. Schneider [43], A. Schopper [42], M. Schubiger [32], S. Schulte [43], M.H. Schune [11],
R. Schwemmer [42], B. Sciascia [23], A. Sciuccati [42], S. Sellam [40], A. Semennikov [38],
M. Senghi Soares [33], A. Sergi [24,k], N. Serra [44], L. Sestini [28], A. Seuthe [15], Y. Shang [5],
D.M. Shangase [78], M. Shapkin [38], I. Shchemerov [38], L. Shchutska [43], T. Shears [54],
L. Shekhtman [38], Z. Shen [5], S. Sheng [4,6], V. Shevchenko [38], B. Shi [6], E.B. Shields [26,m],
Y. Shimizu [11], E. Shmanin [38], R. Shorkin [38], J.D. Shupperd [62], B.G. Siddi [21,i],
R. Silva Coutinho [62], G. Simi [28], S. Simone [19,f], M. Singla [63], N. Skidmore [56], R. Skuza [17],
T. Skwarnicki [62], M.W. Slater [47], J.C. Smallwood [57], J.G. Smeaton [49], E. Smith [44],
K. Smith [61], M. Smith [55], A. Snoch [32], L. Soares Lavra [9], M.D. Sokoloff [59], F.J.P. Soler [53],
A. Solomin [38,48], A. Solovev [38], I. Solovyev [38], R. Song [63], F.L. Souza De Almeida [2],
B. Souza De Paula [2], B. Spaan[15,†], E. Spadaro Norella [25,l], E. Spedicato [20], E. Spiridenkov[38],
P. Spradlin [53], V. Sriskaran [42], F. Stagni [42], M. Stahl [42], S. Stahl [42], S. Stanislaus [57],
E.N. Stein [42], O. Steinkamp [44], O. Stenyakin[38], H. Stevens [15], S. Stone [62,†],

D. Strekalina [38], Y.S Su [6], F. Suljik [57], J. Sun [27], L. Sun [68], Y. Sun [60], P. Svihra [56], P.N. Swallow [47], K. Swientek [34], A. Szabelski [36], T. Szumlak [34], M. Szymanski [42], Y. Tan [3], S. Taneja [56], M.D. Tat [57], A. Terentev [44], F. Teubert [42], E. Thomas [42], D.J.D. Thompson [47], K.A. Thomson [54], H. Tilquin [55], V. Tisserand [9], S. T'Jampens [8], M. Tobin [4], L. Tomassetti [21,i], G. Tonani [25,l], X. Tong [5], D. Torres Machado [1], D.Y. Tou [3], S.M. Trilov [48], C. Trippl [43], G. Tuci [6], N. Tuning [32], A. Ukleja [36], D.J. Unverzagt [17], A. Usachov [33], A. Ustyuzhanin [38], U. Uwer [17], A. Vagner[38], V. Vagnoni [20], A. Valassi [42], G. Valenti [20], N. Valls Canudas [76], M. Van Dijk [43], H. Van Hecke [61], E. van Herwijnen [55], C.B. Van Hulse [40,v], M. van Veghel [32], R. Vazquez Gomez [39], P. Vazquez Regueiro [40], C. Vázquez Sierra [42], S. Vecchi [21], J.J. Velthuis [48], M. Veltri [22,u], A. Venkateswaran [43], M. Veronesi [32], M. Vesterinen [50], D. Vieira [59], M. Vieites Diaz [43], X. Vilasis-Cardona [76], E. Vilella Figueras [54], A. Villa [20], P. Vincent [13], F.C. Volle [11], D. vom Bruch [10], A. Vorobyev[38], V. Vorobyev[38], N. Voropaev [38], K. Vos [74], C. Vrahas [52], J. Walsh [29], E.J. Walton [63], G. Wan [5], C. Wang [17], G. Wang [7], J. Wang [5], J. Wang [4], J. Wang [3], J. Wang [68], M. Wang [25], R. Wang [48], X. Wang [66], Y. Wang [7], Z. Wang [44], Z. Wang [3], Z. Wang [6], J.A. Ward [50,63], N.K. Watson [47], D. Websdale [55], Y. Wei [5], B.D.C. Westhenry [48], D.J. White [56], M. Whitehead [53], A.R. Wiederhold [50], D. Wiedner [15], G. Wilkinson [57], M.K. Wilkinson [59], I. Williams[49], M. Williams [58], M.R.J. Williams [52], R. Williams [49], F.F. Wilson [51], W. Wislicki [36], M. Witek [35], L. Witola [17], C.P. Wong [61], G. Wormser [11], S.A. Wotton [49], H. Wu [62], J. Wu [7], K. Wyllie [42], Z. Xiang [6], Y. Xie [7], A. Xu [5], J. Xu [6], L. Xu [3], L. Xu [3], M. Xu [50], Q. Xu[6], Z. Xu [9], Z. Xu [6], D. Yang [3], S. Yang [6], X. Yang [5], Y. Yang [6], Z. Yang [5], Z. Yang [60], L.E. Yeomans [54], V. Yeroshenko [11], H. Yeung [56], H. Yin [7], J. Yu [65], X. Yuan [62], E. Zaffaroni [43], M. Zavertyaev [16], M. Zdybal [35], M. Zeng [3], C. Zhang [5], D. Zhang [7], L. Zhang [3], S. Zhang [65], S. Zhang [5], Y. Zhang [5], Y. Zhang[57], Y. Zhao [17], A. Zharkova [38], A. Zhelezov [17], Y. Zheng [6], T. Zhou [5], X. Zhou [6], Y. Zhou [6], V. Zhovkovska [11], X. Zhu [3], X. Zhu [7], Z. Zhu [6], V. Zhukov [14,38], Q. Zou [4,6], S. Zucchelli [20,g], D. Zuliani [28], G. Zunica [56]

[1] *Centro Brasileiro de Pesquisas Físicas (CBPF), Rio de Janeiro, Brazil*

[2] *Universidade Federal do Rio de Janeiro (UFRJ), Rio de Janeiro, Brazil*

[3] *Center for High Energy Physics, Tsinghua University, Beijing, China*

[4] *Institute Of High Energy Physics (IHEP), Beijing, China*

[5] *School of Physics State Key Laboratory of Nuclear Physics and Technology, Peking University, Beijing, China*

[6] *University of Chinese Academy of Sciences, Beijing, China*

[7] *Institute of Particle Physics, Central China Normal University, Wuhan, Hubei, China*

[8] *Université Savoie Mont Blanc, CNRS, IN2P3-LAPP, Annecy, France*

[9] *Université Clermont Auvergne, CNRS/IN2P3, LPC, Clermont-Ferrand, France*

[10] *Aix Marseille Univ, CNRS/IN2P3, CPPM, Marseille, France*

[11] *Université Paris-Saclay, CNRS/IN2P3, IJCLab, Orsay, France*

[12] *Laboratoire Leprince-Ringuet, CNRS/IN2P3, Ecole Polytechnique, Institut Polytechnique de Paris, Palaiseau, France*

[13] *LPNHE, Sorbonne Université, Paris Diderot Sorbonne Paris Cité, CNRS/IN2P3, Paris, France*

[14] *I. Physikalisches Institut, RWTH Aachen University, Aachen, Germany*

[15] *Fakultät Physik, Technische Universität Dortmund, Dortmund, Germany*

[16] *Max-Planck-Institut für Kernphysik (MPIK), Heidelberg, Germany*

[17] *Physikalisches Institut, Ruprecht-Karls-Universität Heidelberg, Heidelberg, Germany*

[18] *School of Physics, University College Dublin, Dublin, Ireland*

[19] *INFN Sezione di Bari, Bari, Italy*

[20] *INFN Sezione di Bologna, Bologna, Italy*

[21] *INFN Sezione di Ferrara, Ferrara, Italy*

[22] *INFN Sezione di Firenze, Firenze, Italy*

[23] *INFN Laboratori Nazionali di Frascati, Frascati, Italy*

[24] *INFN Sezione di Genova, Genova, Italy*

[25] *INFN Sezione di Milano, Milano, Italy*

[26] *INFN Sezione di Milano-Bicocca, Milano, Italy*

[27] *INFN Sezione di Cagliari, Monserrato, Italy*

[28] *Università degli Studi di Padova, Università e INFN, Padova, Padova, Italy*

[29] *INFN Sezione di Pisa, Pisa, Italy*

[30] *INFN Sezione di Roma La Sapienza, Roma, Italy*

[31] *INFN Sezione di Roma Tor Vergata, Roma, Italy*

[32] *Nikhef National Institute for Subatomic Physics, Amsterdam, Netherlands*

[33] *Nikhef National Institute for Subatomic Physics and VU University Amsterdam, Amsterdam, Netherlands*

[34] *AGH — University of Science and Technology, Faculty of Physics and Applied Computer Science, Kraków, Poland*

[35] *Henryk Niewodniczanski Institute of Nuclear Physics Polish Academy of Sciences, Kraków, Poland*

[36] *National Center for Nuclear Research (NCBJ), Warsaw, Poland*

[37] *Horia Hulubei National Institute of Physics and Nuclear Engineering, Bucharest-Magurele, Romania*

[38] *Affiliated with an institute covered by a cooperation agreement with CERN*

[39] *ICCUB, Universitat de Barcelona, Barcelona, Spain*

[40] *Instituto Galego de Física de Altas Enerxías (IGFAE), Universidade de Santiago de Compostela, Santiago de Compostela, Spain*

[41] *Instituto de Fisica Corpuscular, Centro Mixto Universidad de Valencia — CSIC, Valencia, Spain*

[42] *European Organization for Nuclear Research (CERN), Geneva, Switzerland*

[43] *Institute of Physics, Ecole Polytechnique Fédérale de Lausanne (EPFL), Lausanne, Switzerland*

[44] *Physik-Institut, Universität Zürich, Zürich, Switzerland*

[45] *NSC Kharkiv Institute of Physics and Technology (NSC KIPT), Kharkiv, Ukraine*

[46] *Institute for Nuclear Research of the National Academy of Sciences (KINR), Kyiv, Ukraine*

[47] *University of Birmingham, Birmingham, United Kingdom*

[48] *H.H. Wills Physics Laboratory, University of Bristol, Bristol, United Kingdom*

[49] *Cavendish Laboratory, University of Cambridge, Cambridge, United Kingdom*

[50] *Department of Physics, University of Warwick, Coventry, United Kingdom*

[51] *STFC Rutherford Appleton Laboratory, Didcot, United Kingdom*

[52] *School of Physics and Astronomy, University of Edinburgh, Edinburgh, United Kingdom*

[53] *School of Physics and Astronomy, University of Glasgow, Glasgow, United Kingdom*

[54] *Oliver Lodge Laboratory, University of Liverpool, Liverpool, United Kingdom*

[55] *Imperial College London, London, United Kingdom*

[56] *Department of Physics and Astronomy, University of Manchester, Manchester, United Kingdom*

[57] *Department of Physics, University of Oxford, Oxford, United Kingdom*

[58] *Massachusetts Institute of Technology, Cambridge, MA, United States*

[59] *University of Cincinnati, Cincinnati, OH, United States*

[60] *University of Maryland, College Park, MD, United States*

[61] *Los Alamos National Laboratory (LANL), Los Alamos, NM, United States*

[62] *Syracuse University, Syracuse, NY, United States*

[63] *School of Physics and Astronomy, Monash University, Melbourne, Australia, associated to [50]*

[64] *Pontifícia Universidade Católica do Rio de Janeiro (PUC-Rio), Rio de Janeiro, Brazil, associated to [2]*

[65] *Physics and Micro Electronic College, Hunan University, Changsha City, China, associated to* [7]

[66] *Guangdong Provincial Key Laboratory of Nuclear Science, Guangdong-Hong Kong Joint Laboratory of Quantum Matter, Institute of Quantum Matter, South China Normal University, Guangzhou, China, associated to* [3]

[67] *Lanzhou University, Lanzhou, China, associated to* [4]

[68] *School of Physics and Technology, Wuhan University, Wuhan, China, associated to* [3]

[69] *Departamento de Fisica, Universidad Nacional de Colombia, Bogota, Colombia, associated to* [13]

[70] *Universität Bonn — Helmholtz-Institut für Strahlen und Kernphysik, Bonn, Germany, associated to* [17]

[71] *Eotvos Lorand University, Budapest, Hungary, associated to* [42]

[72] *INFN Sezione di Perugia, Perugia, Italy, associated to* [21]

[73] *Van Swinderen Institute, University of Groningen, Groningen, Netherlands, associated to* [32]

[74] *Universiteit Maastricht, Maastricht, Netherlands, associated to* [32]

[75] *Tadeusz Kosciuszko Cracow University of Technology, Cracow, Poland, associated to* [35]

[76] *DS4DS, La Salle, Universitat Ramon Llull, Barcelona, Spain, associated to* [39]

[77] *Department of Physics and Astronomy, Uppsala University, Uppsala, Sweden, associated to* [53]

[78] *University of Michigan, Ann Arbor, MI, United States, associated to* [62]

[a] *Universidade de Brasília, Brasília, Brazil*

[b] *Central South U., Changsha, China*

[c] *Hangzhou Institute for Advanced Study, UCAS, Hangzhou, China*

[d] *Excellence Cluster ORIGINS, Munich, Germany*

[e] *Universidad Nacional Autónoma de Honduras, Tegucigalpa, Honduras*

[f] *Università di Bari, Bari, Italy*

[g] *Università di Bologna, Bologna, Italy*

[h] *Università di Cagliari, Cagliari, Italy*

[i] *Università di Ferrara, Ferrara, Italy*

[j] *Università di Firenze, Firenze, Italy*

[k] *Università di Genova, Genova, Italy*

[l] *Università degli Studi di Milano, Milano, Italy*

[m] *Università di Milano Bicocca, Milano, Italy*

[n] *Università di Modena e Reggio Emilia, Modena, Italy*

[o] *Università di Padova, Padova, Italy*

[p] *Università di Perugia, Perugia, Italy*

[q] *Scuola Normale Superiore, Pisa, Italy*

[r] *Università di Pisa, Pisa, Italy*

[s] *Università della Basilicata, Potenza, Italy*

[t] *Università di Roma Tor Vergata, Roma, Italy*

[u] *Università di Urbino, Urbino, Italy*

[v] *Universidad de Alcalá, Alcalá de Henares, Spain*

[†] *Deceased*